CIENTIFIC Publishing Limited

Prevention and Treatment of Natural Disasters

https://ojs.ukscip.com/index.php/ptnd

Article

Assessing the Impact of Climate Change on Glacial Lake Outburst Flood (GLOF) in Eastern Hindu Kush Region Using Integrated Geo -Statistical and Spatial Hydrological Approach

Mariam Sarwar and Shakeel Mahmood *

Department of Geography, Government College University, Lahore 54000, Pakistan
* Correspondence: shakeelmahmoodkhan@gmail.com

Received: 26 April 2024; **Revised**: 30 May 2024; **Accepted**: 7 June 2024; **Published**: 16 July 2024

Abstract: Glacier retreat, a major impact of climate change that continues to occur in many parts of the world, continues to increase the risk of glacial lake outburst floods (GLOFs) in northern Pakistan. The rapid melting of glaciers in the mountains of Northern Pakistan, including the Hindu Kush, the Himalayas and the Karakoram, the rapid melting of glacier has led to the formation of 3044 glacial lakes, with 33 identified as particularly vulnerable to GLOFs. This study uses remote sensing and geographic information systems (GIS) methods for mapping and representing GLOFs. Based on the observational data of lake area, volume, and depth, empirical equations are developed through statistical methods. Only two lakes, Chitral-GL2 and Swat-G31, are classified as lakes with high potential for GLOF. Through modeling techniques using HEC-RAS and HEC-GeoRAS spatial hydrological models integrated with GIS remote sensing, the spatial extent and depth of inundations under different lake volumes are assessed. The analysis reveals that a total area of 20.56 km^2 is susceptible to submersion by GLOFs, with Chitral-GL2 flooding area of 14.80 km^2 and Swat-GL31 5.79 km^2. Different land types are impacted by critical water depths, with built-up and agricultural lands 2.7 km^2 totally, and barren lands 8.93 km^2 under different flood depths ranging from less than 5 m to over 15 m.

Keywords: climate change; flood; GIS; RS; GLOF; HEC-Geo RAS; HEC-RAS; Hindu Kusch

1. Introduction

Globally, recent climate change has led to an increase in the frequency and size of GLOFs [1]. GLOFs are one of severe meteorological disasters that causes damage to human life, infrastructure, and property [2]. The melting of glaciers lead to the development of new water bodies and expansion of existing lakes that can pose a great threat to downstream exposed communities in the case of glacial lake outburst floods. GLOFs are particularly significant as they have the potential to impact areas tens to hundreds of kilometers [3]. The complex combination of environmental and social factors has led to the GLOF disasters [4]. The risk related to GLOFs includes not only the hazards of GLOFs, but can be defined as the product of outburst volume and outburst probability. Temperature changes have a significant influence on glaciers worldwide, particularly in the Hindu Kush Himalayan (HKH) areas. The glaciers are decreasing rapidly, resulting in reduced snow accumulation. Glacier lake outburst floods can cause a significant hazard to vulnerable downstream populations due to the slow formation of new water bodies and the expansion of existing ones. The analysis of the GLOF disasters shows that these events are linked with extreme weather conditions such as rising temperature and intensive rainfall [5,6].

The main source of GLOFs is the failure of lakes blocked by ice or moraine; the latter form between the

frontal positions of receding glaciers and terminal moraine ridges, representing the maximum extent of previous advances [7]. New glacial lakes are being formed, old moraine-dammed lakes are being extended, and the probability of GLOFs is rising as a result of rapid glacier melting. The Himalayan region's temperatures are predicted to increase by 1 to 6 °C in 2100 by the Intergovernmental Panel on Climate Change (IPCC) [8]. Given that increased glacier loss may eventually affect millions of people, high mountain areas in Asia are prioritized as particularly susceptible to climate change [9]. The Hindu Kush region is also characterized by the widespread presence of such glacial lakes, many of which pose potential flooding risks [10]. Eastern Hindu Kush region is prone to geological and hydro-meteorological disaters and has experienced major GLOFs in more than 8000 glacial lakes and 209 potentially hazardous glacial lakes (PDGLs), 52 of which are in Pakistan, have been found in the Hindu Kush by previous studies [6,11].

The International Center for Integrated Mountain Development (ICIMOD) released glacier and sea level statistics in 2005, demonstrating that the Hindu Kush Himalayan (HKH) region were warmer than the global average level. The study identified all 2420 known glacial lakes in 10 rivers; the largest amount of freshwater is found in the Indus Basin (574), and the Gilgit River Basin (614). 380 out of 614 glacial lakes along the Gilgit River have been classified as large glacial lakes [12].

The GLOF risk is directly proportional to the exposed elements. In 1986, the International Centre for Integrated Mountain Development (ICIMOD) actively carried out an inventory of glaciers and glacial lakes, as well as the identification of potential problematic glacial lakem [13]. Glacial lake temporal mapping can be used as an indication to track shifting climatic trends [14]. GLOF risk and hazard evaluations, modelling history, and possible GLOFs in the future have been the subject of several research conducted globally [15]. High mountain regions often face the risk of glacial disasters worldwide. The recent disasters in Himalayan have demonstrated this, causing deaths and significant damage to infrastructure that disrupt people's daily life [16].

Natural disasters, such as snow avalanches, GLOFs, and landslides, are common in this area [17]. The destabilization of glaciers, especially in the Karakoram Mountains has caused several glacial lakes with a high risk of GLOF. In the Himalayas, the severity of GLOF varies, occurring every three to ten years. A comprehensive analysis and evaluation of the consequences of future GLOF disasters in the Great Lakes region is of great significance, especially in the context of climate change [18]. In particular, Hindu Kush-Karakoram-Himalayan regions have experienced more frequent floods and flood-induced secondary disasters in recent years [19]. Among these catastrophic events, most GLOFs events happened in the Karakoram region of Gilgit Baltistan, mainly due to heavy rains, sudden temperature rise, and heat wave [20]. The Latest events include the DLOFs from 2007 and 2008 on the Passu Glaciers [21]. In 2003 and 2008–2017, due to the sudden rupture of the supraglacial glacial lake in the Gurkin Valley and other reasons, the Reshun Valley experienced GLOF. Another area quite vulnerable to flooding because of the migration of the Muchowar and Shisper glaciers is the Hassanabad Basin [22]. The Hassan Abad Basin has experienced five minor events between 1890 and 1905 [23]. Recently, three major GLOF events were observed in 2019 and 2020 [24]. The most recent Chamoli catastrophe occurred on 7 February 2021, causeing the death of more than 150 people [25], amd the inundation of surrounding rivers, impacting the river water [26].

There are the records of documented cases of GLOFs across the world. In 1941, the Peruvian city of Huaraz was destroyed by a flood, killing 4500 people [27]. In 1968–1970, explosives from Swiss high mountain lakes caused debris and significant damage in the town of Saas Balen [28]. The 1968 event alone swept through about 400,000 m^3 of debris. The main objective of this study is to analyze the extent of GLOF impact on downstream by using remote sensing/GIS and hydrological techniques.

2. Study Area

The focus of the study is on the eastern region of Hindu Kush in northwestern Pakistan. Geographically, the eastern part of Hindu Kush extends from 34°34'11" N to 36°54'30" N, and from 71°11'56" E to 73°52'5" E (Figure 1). The districts of Chitral, Upper Dir, Lower Dir, and Swat make up Eastern Hindu Kush. Physically, it is characterized by two mountain ranges: the eastern and western ranges [29]. The Kabul basin is divided by the western range, and the Swat basin is divided by the eastern range. These snow-capped mountains have several glaciers in valleys at an altitude of 4000 m above sea level [30]. The climate of the study area changed from cool to warm, with temperatures ranging from 16 °C and 32 °C. Typically from December to February, wintertime

temperatures drop below freezing, and snowfall is a common sight. There is a range of 823 to 2149 mm of annual precipitation. When the weather gets cold, snowfall often starts in November and lasts until December [31]. Snow melting starts in March and continues depending on elevation.

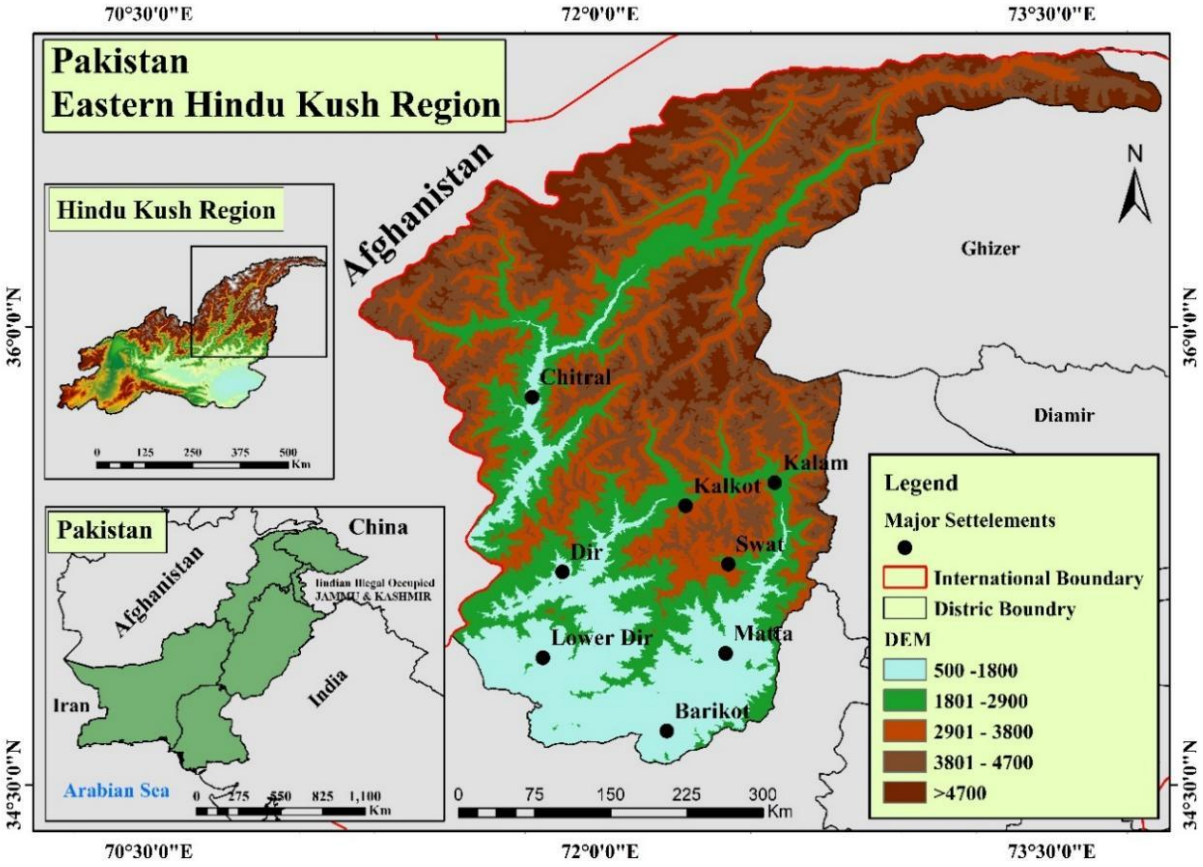

Figure 1. Location of Study Area.

3. Research Methodology

The study utilized Advanced Spaceborne Thermal Emission and Reflection Radiometer Global Digital Elevation Model (ASTER GDEM) with Landsat imagery at a 30-metre elevation and Sentinel-2 with a 10-metre elevation imagery are available from the United States Geological Survey (USGS) open-source geospatial database. Meteorological data covering the period from 1991 to 2019 was acquired from the Regional Meteorological Center in Lahore. Population data was sourced from the Pakistan Bureau of Statistics.

Remotely sensed data served two primary purposes: firstly, assess temperature and rainfall variations in the Hindu Kush region, and secondly, identify the effects of rainfall and temperature on glacial lakes.

3.1. Lake Discharge Estimation

Historically, various empirical formulas have been employed to estimate lake discharge following collapses of natural dams (such as moraines or bedrock dams). Inputs for these calculations usually include lake area, volume, dam height, and water depth. For example, the peak discharge (Q_{max}) caused by the failure of an ice-dammed lake, as observed in Keara, was estimated by using Walder and Costa's (1988) equation for floods that are not tunneled, in Equation (1).

$$Q_{max} = 1100 \times (V/10^6)^{0.44} \quad (1)$$

3.2. Satellite Image Classification

Firstly, in order to classify satellite images, a suitable categorization technique for the study area must be used. As a result, this study identified many types of Land use/Land Cover (LULC) through a modified classification technique. Satellite imaging pixels were categorized by using supervised classification according to comparable or identical spectral reflectance properties [32]. To detect LULC in the 200 Landsat pictures, the supervised classification strategy used the maximum likelihood algorithm in ERDAS images. The three Steps in the classification process are selection, classification, and evaluation or accuracy assessment of the training sample. There are about fifty training examples ready for each lesson and eighty training examples given on each map.

The maximum likelihood technique is the most popular and extensively utilized parametric classifier for examining changes in LULC [33]. The multidimensional space of each class sample's cell is determined by applying Bayes' theorem, which forms the basis of the maximum likelihood classification framework [34].

3.3. Spatial Hydrological Modeling

The Hydrologic Engineering Center of the US Army Corps of Engineers developed the Geographical River Analysis System (HEC-GeoRAS or HEC-RAS). Figure 2 shows the river geometry GIS data may be prepared for input into HECRAS, which is subsequently used to create the final inundation map, using a number of techniques, tools, and utilities included in the HEC-GeoRAS GIS extension.

Triangular Irregular Network (TIN), digital elevation model (DEM), and land use are required inputs for river geometry preparation using the HEC-GeoRAS model. The water level elevation along a river is determined by HEC-RAS by using stream flow data and the river geometry file.

The HEC-GeoRAS interface should be used to digitize the river stream centerline, bank lines, flow route centerlines, and XS cut lines from a previous river file, aerial photos, or topographical data. The geographic database files saved in HEC-GeoRAS include river reach (river segment between junctions), cross-sections, and other related data. All other attributes are obtained automatically by HEC-GeoRAS; however, the river and cross-section data layers are built by using predefined attribute tables that are manually input for the river and reach names.

The interface collects geometric data in an *xml* format, which is then loaded into HEC-RAS. The simulation results of the HEC-RAS model will be transferred into the GIS environment, and the HEC-GeoRAS tool will be used for further research. The *sdf* format is used for the GIS data that is transferred between ArcGIS and HEC-RAS. The HEC-RAS editing tools may be used to modify the output GIS geometric data in the model. A total of 67 cross sections are drawn perpendicular to the streamlines at 1000 m intervals at a depth of 1500 m.

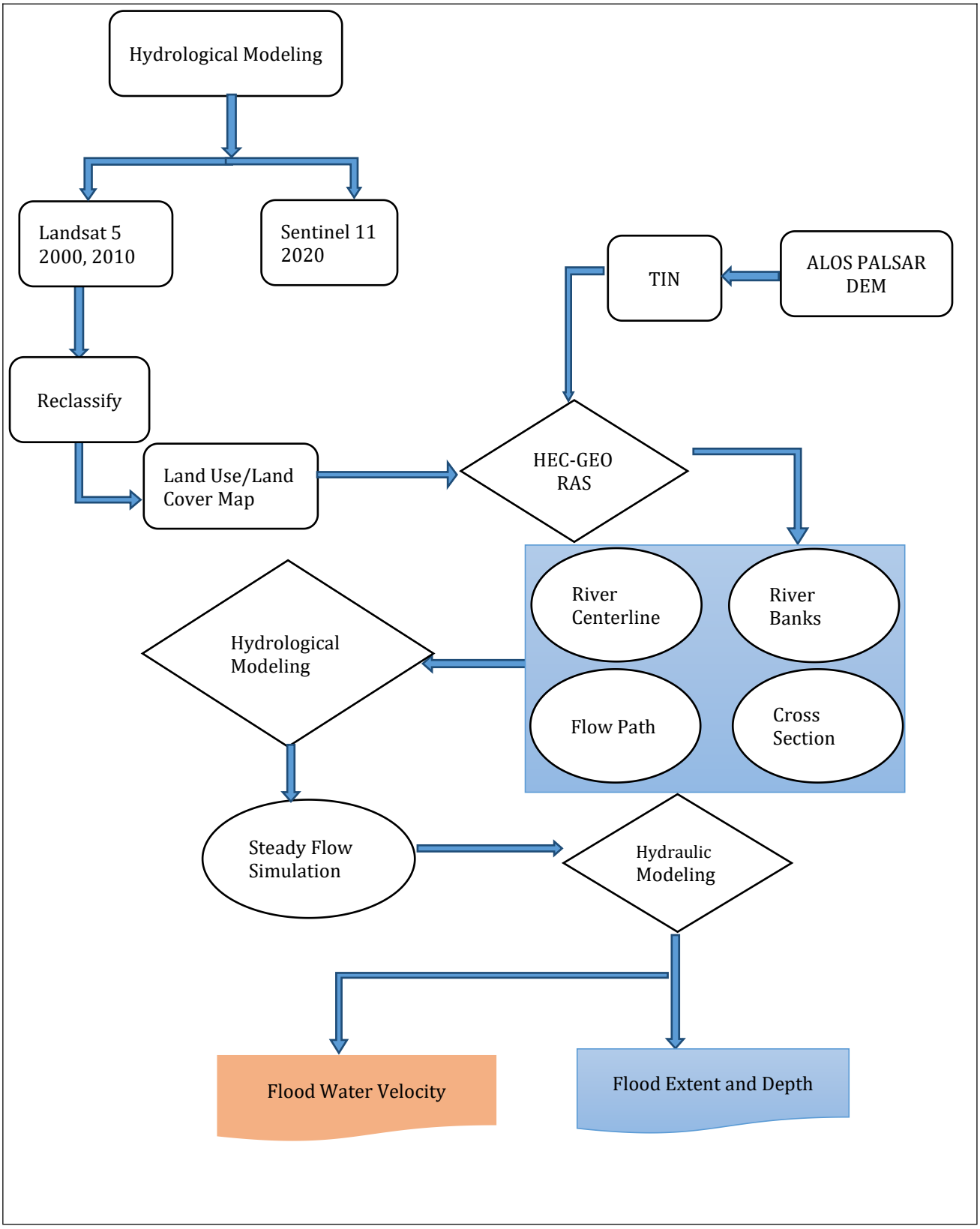

Figure 2. Spatial Hydrological Modeling.

4. Analysis, Result and Discussion

4.1. Climate Change Impact on Glacial Lakes

The climate of the eastern Hindu Kush is classified as semi-arid to arid, with little precipitation and humidity and high temperatures [35]. The location lies under the Himalayan rain shadow and receives little monsoonal precipitation. Drosh and Chitral get an average of 600 and 450 mm of precipitation per year, respectively, with the majority falling in the spring and winter. Summer and autumn are often dry, with just 10–25 mm of rainfall each month. While the average summer and winter temperatures in the southern foothills are around 30 and 18 °C, the mean temperature in summer in the central valley of the the Himalayas is between 15 and 25 °C, as shown in Figure 3.

During the time of heavy rains in the Hindu Kush area, new lakes arise as well as old lakes merge and expand. These two lakes are located in a region with heavy rainfall.

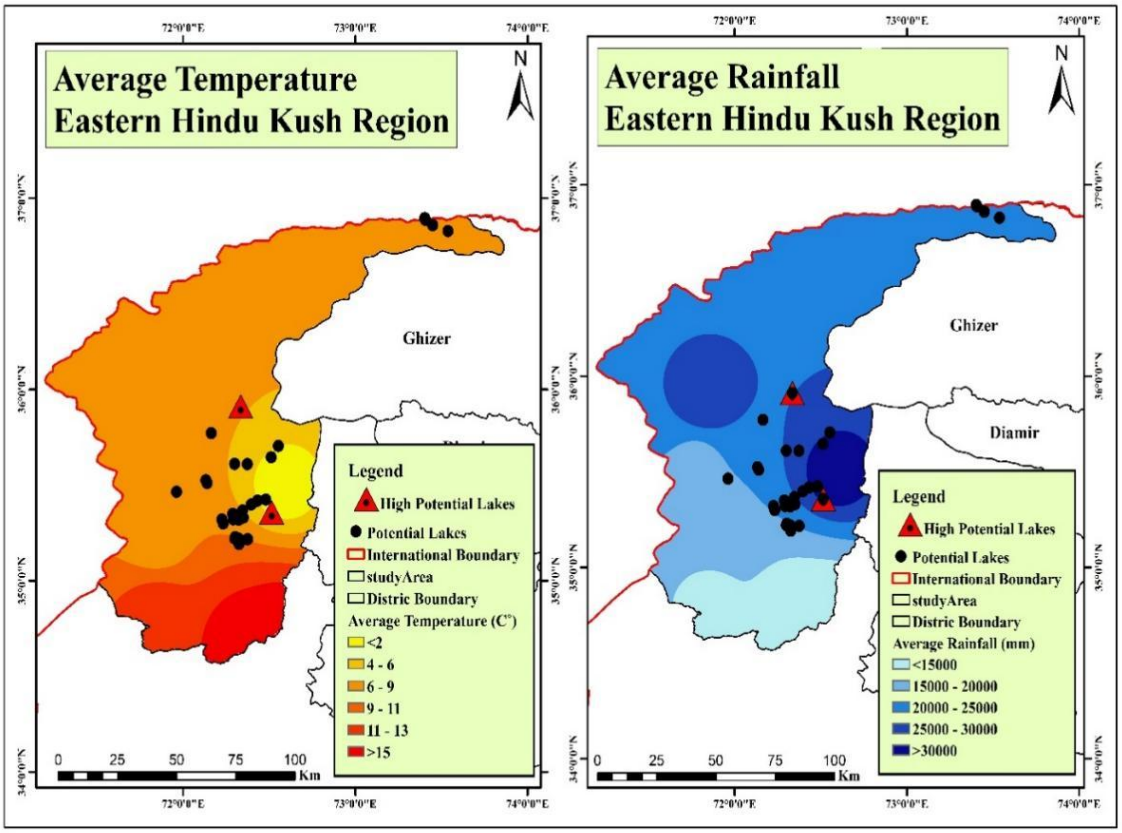

Figure 3. Spatial pattern of average rainfall (mm) and temperature (°C) of Eastern Hindu Kush (1991–2020).

The temperature is maximum in July and minimum in January. The total average of maximum temperature showed that June is the hottest month in the last 10 years with the temperature of 36.6 °C whereas January is the coldest month with the temperature of 9.9 °C. The temperature variation could be clearly seen in Figure 4. Lowe Dir Upper Dir and Sidhu Sharif show the highest temperature.

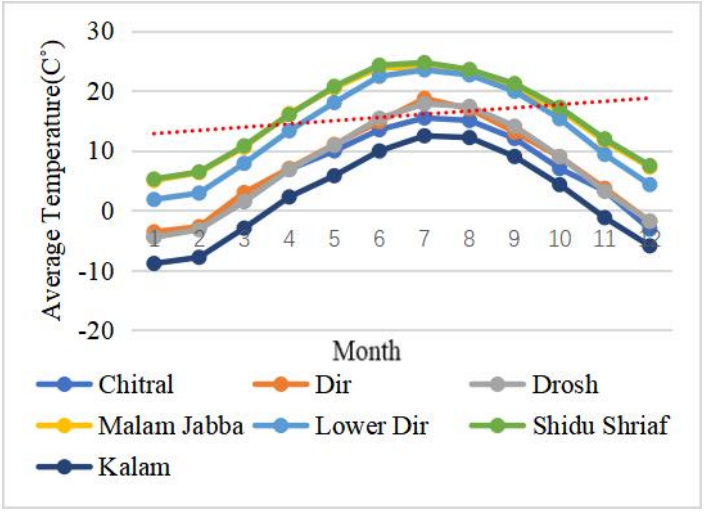

Figure 4. Average temperature (°C) of the Eastern Hindu Kush region.

The rainfall trend could be seen in Figure 5, with more rainfall in January, February, March, and November, while less rainfall in June, July, August, and October. The rainfall in March and November is the highest. Generally, there is more rainfall in January, February, and March. The analysis of ten-year data reveals that the rainfall patterns in January, April and May show a downward trend, while in November they show an upward trend.

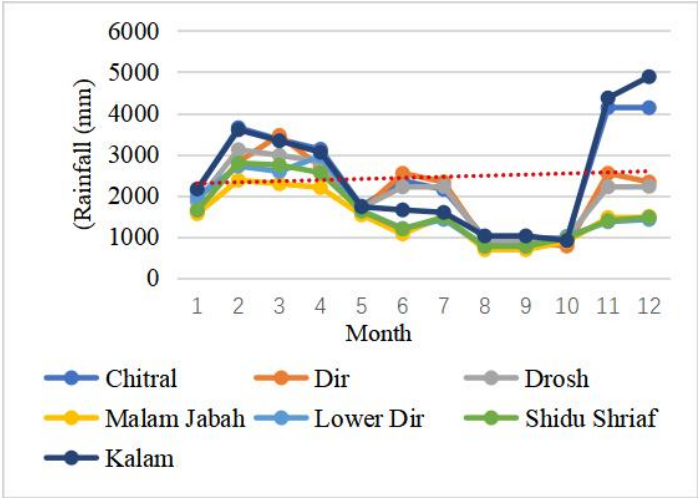

Figure 5. Average rainfall (mm) of the Eastern Hindu Kush region.

4.2. GLOF Modelling Using Spatial Hydrological Approach

The geometric data (Figure 6) shows that the unsteady flow conditions were input into HEC-RAS and the simulation was carried out. In HEC-RAS, after the analysis of unsteady flow, these data were used for the development of flood maps. The data were input into the ArcGIS environment to produce maps. The flood polygons were overlaid with infrastructure data (collected in the field) and identified infrastructure at risk of possible flood zones.

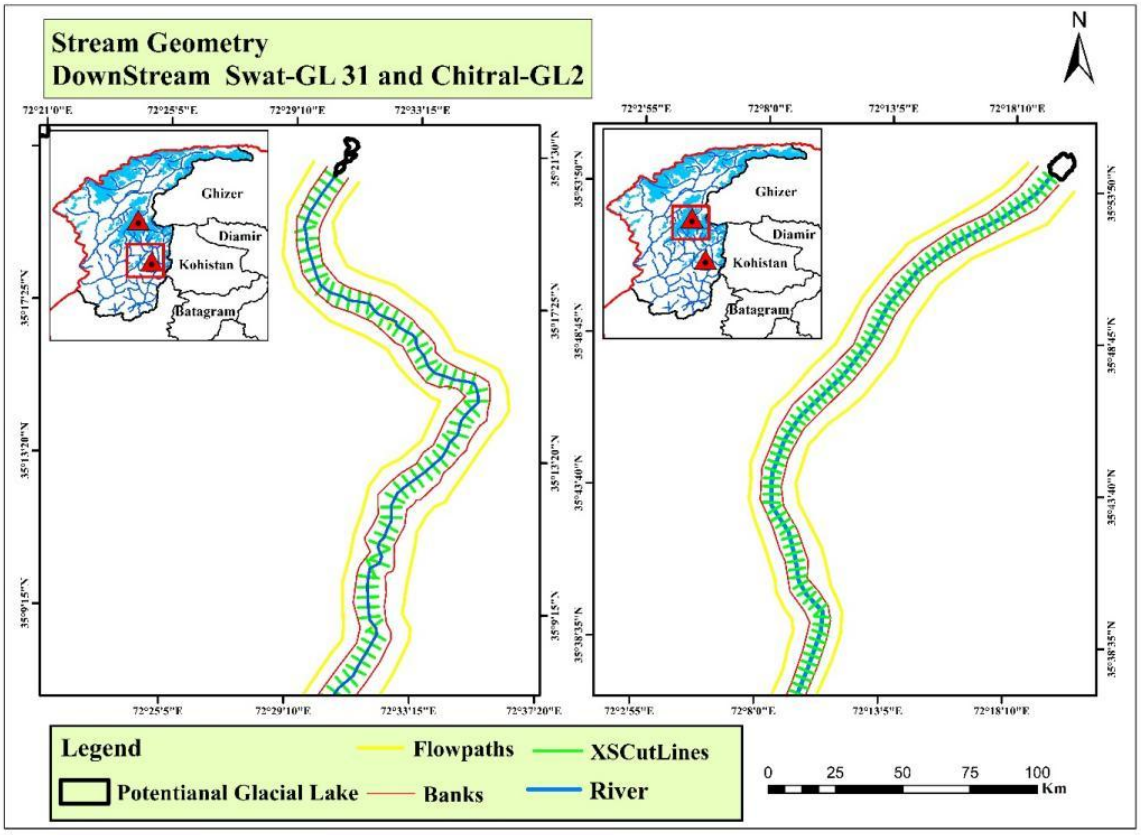

Figure 6. Stream geometry extracted from digital elevation model.

4.3. Spatial Extent of Estimated Floods

The spatial extent of flood peaks with Lake Volume is variable along the selected reach of Chitral-GL2. The extent of flood decreases towards downstream shown as Figure 7. In the selected reach, upper section of 3.08Km is wide having narrow particularly over the right bank and deep with average width of 0.142 km and the middle section of 2.26 km is narrow and deep the lower section of 1 km wide is also narrow and depth with average width of 0.046 km. Total 14.86 km2 area submerge Chitral-GL2 the extent and depth of Swat-GL31 flood depth is 5–10 m. the upper section flood extend is 1.1 km wide having narrow. The middle section of 1.0 km and lower section is 1.5 km wide and narrow depth. Total 5.79 km2 area submerge in Swat-GL31.

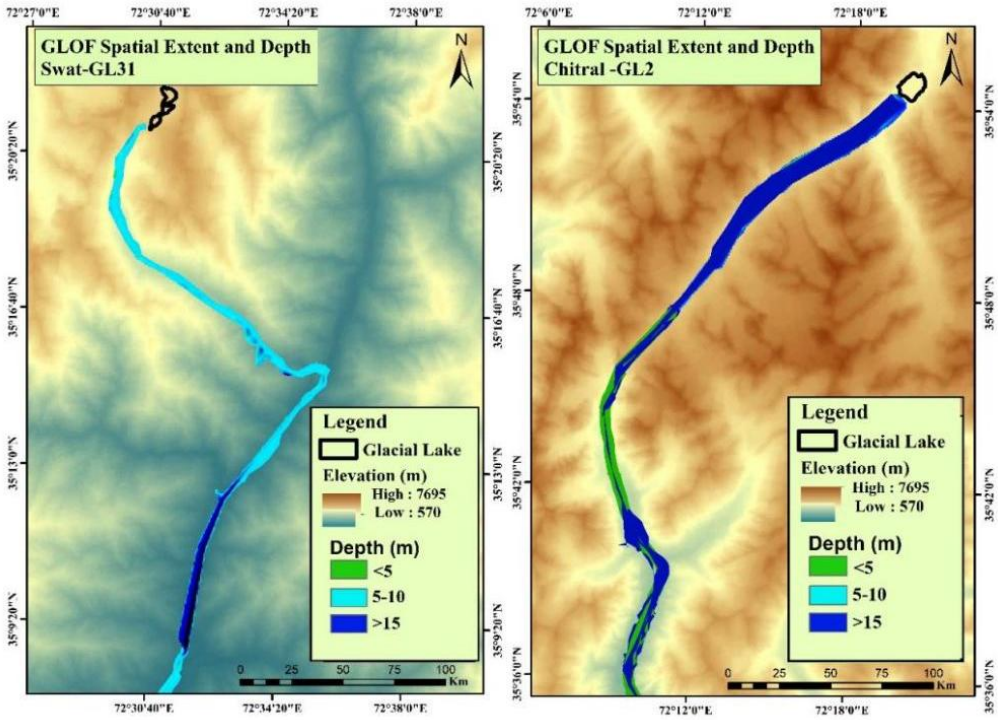

Figure 7. Spatial extent and vertical profile of estimated GLOF.

4.4. Velocity of Estimated Flood

The peak flood velocity map (Figure 8) illustrates the risk of high-intensity flooding close to the channel, whereas downstream regions seem to experience lower-intensity flooding. This is because of the channel's breadth. In Swat GL31, the flood are is 10.42 km^2, whereas in Chitral GL2, it is 12.36 km^2.

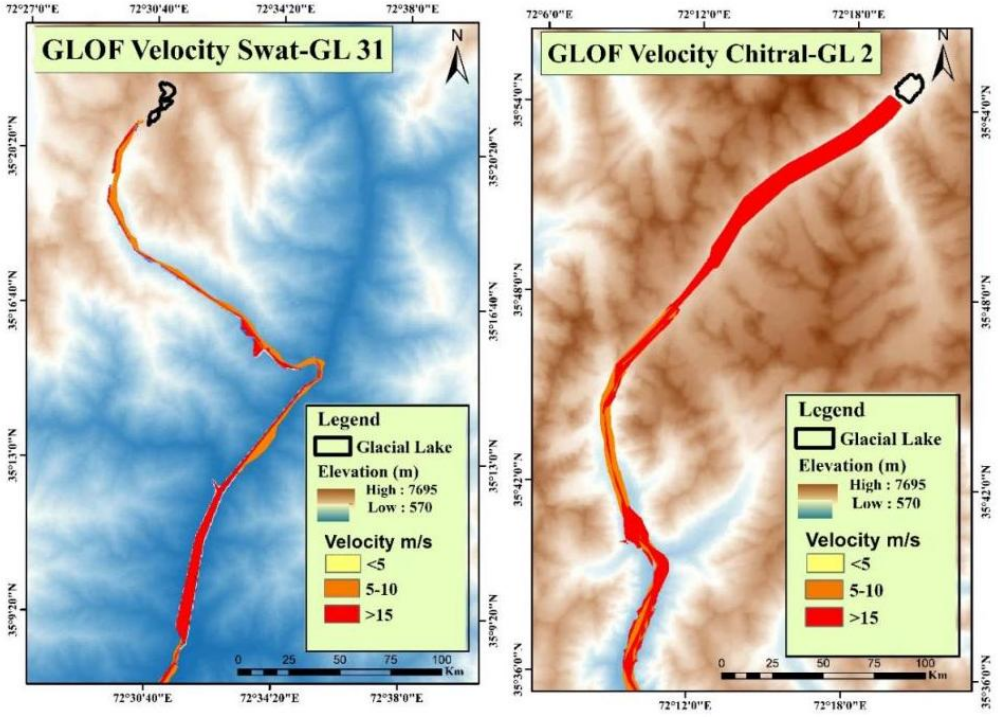

Figure 8. Flow velocity of estimated flood Swat-GL31 and Chitral-GL2.

According to Figure 9, Agriculture (2504.52 km^2, 23.75% of the total studied area) is the largest land use group, and Builtup (2840.34 km^2, 26.93% of the total area) is the second-largest land use group. The other land use classifications are Barren Land (3589.53 km^2, 34.04% of the total area), and Water (1609.36 km^2, 15.26% of the total area).

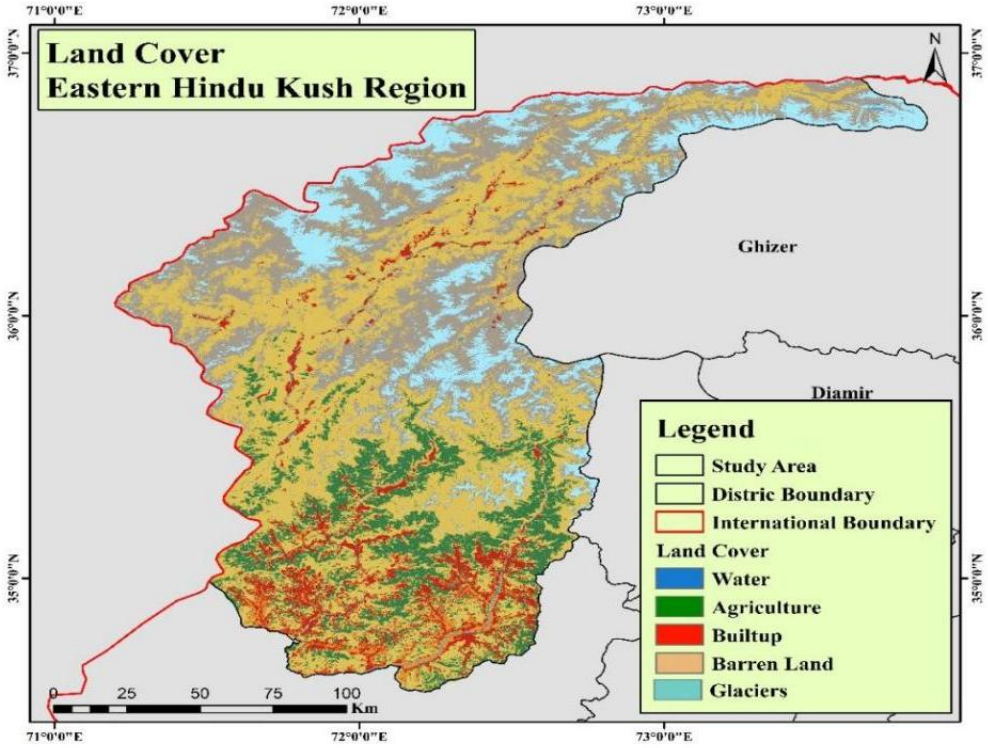

Figure 9. Land cover of Eastern Hindu Kush.

Table 1 shows the summary of flood effect area in km^2 and the proportion in %, downstream flood. A total area of 20.56 km^2 was assessed to be flooded at different depth. About 2 km^2 builtup and agricultural land was calculated to be flooded in two flood scenarios. Similarly, 8.93 km^2 of barren land was expected to be flooded.

Table 1. Estimated land covers exposed to GLOF in Eastern Hindu Kush.

Serial No.	Land Cover	Area (km^2)	Proportion (%)
1	Agriculture	2.70	13.13
2	Water	6.93	33.70
3	Barren land	8.93	43.43
4	Builtup	2.00	9.74

Figure 10 shows the same result that because of the low-gradient downstream, the crucial depth of flood affects most types of land. A total area of 20.56 km^2 was assessed to be flooded at different depths. Builtup and Agricultural land of about 2 km^2 was calculated to be flooded in two flood scenarios. Similarly, 8.93 km^2 barren land was expected to be flooded at depths ranging from 5 m to 15 m.

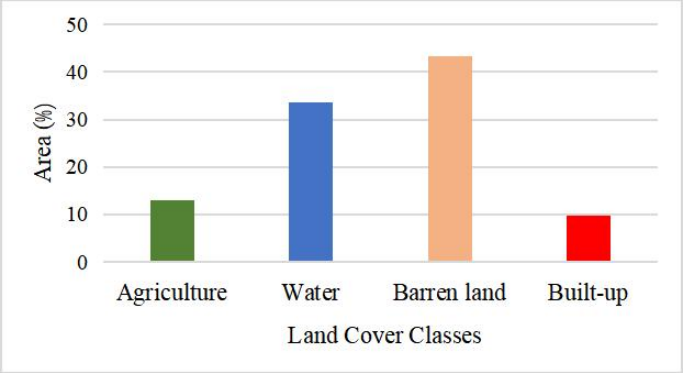

Figure 10. Estimated land cover exposed to GLOF in Eastern Hindu Kush.

5. Discussion

This study utilized remote sensing data sets and GIS techniques, and HCE-RAS hydraulic modelling to examine the GLOF event in Eastern Hindu Kush. Additionally, risk assessment methodology was created to determine the glacial lake's downstream flood. In particular, the total surface area of glacial lakes expanded from 9.72 km^2 to 12.36 km^2 between 2000 and 2020, despite the fact that there were 101 glacial lakes in 2000. Of them, 31 were identified as Potentially Dangerous Glacial Lakes (PDGL), 16 in Swat, 9 in Upper Dir, and 6 in Chitral. Two lakes, with estimated depths of 41.86 m and 30.43 m, were designated as high potential glacial lakes and downstream flood risk area identified through HEC-RAS. Figure 2 shows the detail methodology of Hydrological Modeling. Figure 3 shows the spatial pattern of average rainfall (mm) and temperature (°C) of Eastern Hindu Kush under the Himalayan rain shadow, receiving little monsoonal precipitation. Drosh and Chitral get an average of 600 and 450 mm of precipitation per year, respectively, with most falling in the spring and winter. It is often dry in summer and autumn, with just 10–25 mm of rainfall each month. Figure 4 shows that the average temperature (°C) of the Eastern Hindu Kush region is maximum in July, whereas it is minimum in January. The total average of maximum temperature shows that June is the hottest month in the last 10 years with the temperature of 36.6 °C, whereas January is the coldest month with the temperature of 9.9 °C. The rainfall trend could be seen in Figure 5, with more rainfall in January, February, March, and November, and less rainfall in June, July, August, and October. The rainfall in March and November is the highest in history. Generally, January, February and March receive more rainfall. The analysis of ten-year data reveals that there is a decreasing trend in the rainfall patterns in May, April and January, but an increasing trend in November. Figure 6 Shows the geometric data and unsteady flow conditions were input into HEC-RAS and the simulation was carried out. In HEC-RAS, after the analysis of unsteady flow, these data were used for the development of flood maps. The data were input into the ArcGIS environment to produce maps.

Figure 7 shows that the upper portion of the selected reach, spanning 3.08 km, has become wide from narrow, particularly below the right bank, which is deep and narrow with an average width of 0.142 km^2. The center part, which is 2.26 km^2 broad and deep, is similarly deep and narrow, with an average width of 0.046 km^2. A total area of 14.86 km^2 is submerged in Chitral-GL 2. The extent and depth of the Swat-GL31 flood is thin, with a depth mostly ranging from 5 to 10 meters. The upper section of the flood extends to 1.1 km in width, remaining narrow. The middle section spans 1.0 km^2, while the lower section covers 1.5 km^2, both being wide and narrow in depth. A total area of 5.79 km^2 was submerged in Swat-GL31.

Figure 8 illustrates the risk of high-intensity flooding close to the channel, whereas downstream regions seem to experience lower-intensity flooding. According to Figure 9, Green Cover, which comprises 2504.52 km^2 (23.75% of the total studied area), is the largest land use group. Built-up areas, covering 2840.34 km^2 (26.93% of the total area), form the second-largest land use group. Other land use classifications include Barren Land (3589.53 km^2, 34.06% of the total area) and Water (1609.36 km^2, 15.26% of the total area).

Table 1 and Figure 10 show similar results, indicating that due to the low-gradient downstream, the crucial depth of the flood affects most types of land. A total area of 20.56 km^2 was assessed to be flooded at different depths. Built-up and agricultural land of about 2 km^2 was calculated to be flooded in two flood scenarios. Similarly, 8.93 km^2 of barren land was expected to be flooded at depths ranging from 5 to 15 meters.

It is imperative to prioritize further research efforts to better understand and mitigate the risks associated with GLOFs, including comprehensive monitoring of glacier retreat, lake expansion, and potential triggering events. Implementing proactive measures, such as early warning systems and community-based disaster preparedness initiatives, is essential to enhance resilience and reduce the potential impact of future GLOF events on vulnerable communities in the region.

Continuous monitoring of these glacial lakes and their vulnerability to GLOFs is critical due to continuous climate change. In response to recognized climate fluctuation in the area, the frequency and magnitude have grown during the last three decades [36,37]. Global warming has long been recognized as a cause of glacier melting [38]. Since the end of the Little Ice Age, the average surface temperature on Earth has risen. Temperatures have risen by 0.3 °C–0.6 °C during the past century. The Intergovernmental Panel on Climate Change (IPCC) anticipated that temperatures in the Himalayas will climb by 1 °C to 6 °C from 2100 [7,39]. Previous studies have revealed that high-intensity flooding affects 40% of the Hindu Kush Karakorum and Himalayas, causing property damage possibly [40]. The potential of InSAR technology to identify shifts in slope and instability in moraine dams makes it valuable [41]. We recommend frequent and continuous monitoring of the lake and its adjacent areas.

Furthermore, the utilization of the HEC-RAS 1-D steady-flow hydraulic model allows for the simulation of GLOF events and the routing of GLOF hydrographs to downstream locations, aiding in defining flood characteristics. Data analysis and the outcomes of the simulation indicate that in the Eastern Hindu Kush, glaciers are retreating rapidly, causing the expansion of lakes at an unprecedented pace and posing imminent dangers to settlements.

The GLOF phenomena occurs in mountainous regions worldwide, causing significant damage to property, infrastructure, and life in the downstream. Therefore, it is imperative to conduct thorough research to better understand GLOFs and develop strategies to mitigate their impacts. Specifically, detailed studies examining the capacity of lake outlets and the development of relocation strategies for households at risk are strongly recommended to enhance preparedness and resilience for future GLOF events.

6. Conclusions

In conclusion, the study reveals that a significant area of 20.56 km^2 is susceptible to submersion by glacial lake outburst floods (GLOFs) based on the flood scenario analyzed. The velocity of the flood in Chitral-GL2 is notably higher compared to Swat-GL31 due to the steeper floodplain gradient of Chitral-GL2 in contrast with Swat-GL31. Specifically, an area of 14.80 km^2 in Chitral-GL2 is inundated, while the area in Swat-GL31 is 5.79 km^2.

The analysis highlights the critical impact of flood depth on various land types, particularly affecting built-up and agricultural lands totaling 2.7 km^2 and barren lands spanning 8.93 km^2 under different flood depth scenarios ranging from less than 5 m to 15 m.

Moreover, the findings underscore the alarming pace at which glaciers are retreating and lakes are expanding, posing imminent hazards to settlements. Particularly in the northern regions, unstable slopes present additional risks, with potential triggering events such as avalanches or earthquakes exacerbating the likelihood of GLOFs.

7. Recommendations

The following are suggestions for the above conclusions.

Regular monitoring of glaciers and glacial lakes, as well as adaptation measures such as early warning systems and mitigation, are necessary in areas susceptible to Glacial Lake Outburst Floods (GLOFs). To control GLOFs, it is essential to reduce temperatures to slow glacial melting. Areas prone to flooding should be identified, and the construction of houses, roads, and other infrastructure near these areas should be avoided. Field surveys can be conducted to fully understand the mechanisms of dam collapses and GLOFs.

Constructing dams for the gradual release of water can help reduce the impacts of floods. Raising awareness among people about flood risks can help prevent the destruction of crops. The Ministry of Environment and the National Disaster Management Authority (NDMA) are improving risk mapping, early warning systems, and disaster prevention planning, including GLOF risk recording and management at village and district levels.

Local planning and long-term development programs in the region should place greater importance on research and development, aim to limit the exposure of human settlements to GLOFs, and increase communication and participation of the local population. In the Eastern Hindu Kush region, GLOFs have caused severe damage. The damages were not only caused by the discharge of water but also by debris flow and silt deposits. To minimize potential damages in the future, it is essential to monitor the downstream floodplain and its geomorphology. High-resolution images can be used to identify glacial lakes for further investigation using the AHP (Analytic Hierarchy Process) method.

The findings of this study can help the Provincial Disaster Management Authority (PDMA), National Disaster Management Authority (NDMA), Soil Department, and Irrigation Department develop methods to reduce GLOF risks.

Author Contributions

M.S. and S.M.: conceptualization; methodology; software; validation; formal analysis. M.S.: original draft preparation. S.M.: writing—review and editing. M.S.: visualization. S.M.: supervision.

Funding

This work received no external funding.

Institutional Review Board Statement

Not applicable.

Informed Consent Statement

Not applicable.

Data Availability Statement

Data will made available on request

Conflicts of Interest

The authors declare no conflict of interest.

References

1. Rahman, A. U.; Shaw, R. Floods in the Hindu Kush Region: Causes and Socio-Economic Aspects. In *Mountain Hazards and Disaster Risk Reduction*, 1st ed.; Nibanupudi, H.K., Shaw, R., Eds.; Springer: Tokyo, Japan, 2015; pp. 33–52. [CrossRef]
2. Emmer, A. Geomorphologically Effective Floods from Moraine-Dammed Lakes in the Cordillera Blanca, Peru. *Quat. Sci. Rev.* **2017**, *177*, 220–234. [CrossRef]
3. Vilca, O.; Mergili, M.; Emmer, A.; Frey, H.; Huggel, C. The 2020 glacial Lake Outburst Flood Process Chain at Lake Salkantaycocha (Cordillera Vilcabamba, Peru). *Landslides* **2021**, *18*, 2211–2223. [CrossRef]
4. Bazai, N.A.; Cui, P.; Carling, P.A.; Wang, H.; Hassan, J.; Liu, D.; Zhang, G.; Jin, W. Increasing Glacial Lake Outburst Flood Hazard in Response to Surge Glaciers in the Karakoram. *Earth-Sci. Rev.* **2021**, *212*, 103432. [CrossRef]
5. Nie, Y.; Liu, Q.; Wang, J.; Zhang, Y.; Sheng, Y.; Liu, S. An Inventory of Historical Glacial Lake Outburst Floods in the Himalayas Based on Remote Sensing Observations and Geomorphological Analysis. *Geomorphology* **2018**, *308*, 91–106. [CrossRef]
6. Bajracharya, B.; Shrestha, A.B.; Rajbhandari, L. Glacial Lake Outburst Floods in the Sagarmatha Region. *Mt. Res. Dev.* **2007**, *27*, 336–344. [CrossRef]
7. Paul, F.; Kääb, A.; Haeberli, W. Recent Glacier Changes in the Alps Observed by Satellite: Consequences for Future Monitoring Strategies. *Global Planet. Change* **2007**, *56*, 111–122. [CrossRef]
8. Harrison, S.; Kargel, J.S.; Huggel, C.; Reynolds, J.; Shugar, D.H.; Betts, R.A.; Emmer, A.; Glasser, N.; Haritashya, U.K.; Klimeš, J.; et al. Climate Change and the Global Pattern of Moraine-Dammed Glacial Lake Outburst Floods. *Cryosphere* **2018,** *12*, 1195–1209. [CrossRef]

9. Hock, R.; Bliss, A.; Marzeion, B.E.N.; Giesen, R.H.; Hirabayashi, Y.; Huss, M.; Radić, V.; Slangen, A.B. GlacierMIP–A Model Intercomparison of Global-Scale Glacier Mass-Balance Models and Projections. *J. Glaciol.* **2019**, *65*, 453–467. [CrossRef]
10. Schmidt, S.; Nüsser, M.; Baghel, R.; Dame, J. Cryosphere Hazards in Ladakh: The 2014 Gya Glacial Lake Outburst Flood and Its Implications for Risk Assessment. *Nat. Hazards* **2020**, *104*, 2071–2095. [CrossRef]
11. Ashraf, A.; Naz, R.; Roohi, R. Glacial Lake Outburst Flood Hazards in Hindukush, Karakoram and Himalayan Ranges of Pakistan: Implications and Risk Analysis. *Geomatics, Nat. Hazards Risk* **2014**, *3*, 113–132. [CrossRef]
12. Bajracharya, S.R.; Maharjan, S.B.; Shrestha, F.; Guo, W.; Liu, S.; Immerzeel, W.; Shrestha, B. The Glaciers of the Hindu Kush Himalayas: Current Status and Observed Changes from the 1980s to 2010. *Int. J. Water Resour. Dev.* **2015**, *31*, 161–173. [CrossRef]
13. Inventory of Glaciers, Glacial Lakes and Glacial Lake Outburst Floods: Monitoring and Early Warning Systems in the Hindu Kush Himalayan Region Bhutan. Available online: https://lib.icimod.org/record/21962 (accessed on 1 November 2020).
14. A Monitoring of Mountain Glacial Variations in Northern Pakistan, from 1992 to 2009 Using Landsat and ALOS Data. Available online: https://www.researchgate.net/publication/241277263_Monitoring_of_Mountain_Glacial_Variations_in_Northern_Pakistan_from_1992_to_2009_using_Landsat_and_ALOS_data (accessed on 1 November 2020).
15. Allen, S.K.; Sattar, A.; King, O.; Zhang, G.; Bhattacharya, A.; Yao, T.; Bolch, T. Glacial Lake Outburst Flood Hazard under Current and Future Conditions: Worst-Case Scenarios in a Transboundary Himalayan Basin. *Nat. Hazards Earth Syst. Sci.* **2022**, *22*, 3765–3785. [CrossRef]
16. Meena, S.; Bhuyan, K.; Chauhan, A.K.; Singh, R.P. Snow Covered with Dust after Chamoli Rockslide: Inference Based on High-Resolution Satellite Data. *Remote Sens. Lett.* **2021**, *12*, 704–714. [CrossRef]
17. Reynolds, J.M. Managing Glacial Hazards for Hydropower Development in the Himalayas, Hindu Kush and Karakoram. In Proceedings of the ASIA 2014, Colombo, Sri Lanka, 11–13 March 2014.
18. Mondal, S.K.; Patel, V.D.; Bharti, R.; Singh, R.P. Causes and Effects of Shisper Glacial Lake Outburst Flood Event in Karakoram in 2022. *Geomatics, Nat. Hazards Risk* **2023**, *14*, 2264460. [CrossRef]
19. Wester, P.; Mishra, A.; Mukherji, A.; Shrestha, A.B. *The Hindu Kush Himalaya Assessment: Mountains, Climate Change, Sustainability and People*, 1st ed.; Springer Nature: Cham, Switzerlan, 2019; 627p. [CrossRef]
20. Ashraf, A.; Iqbal, M.B.; Mustafa, N.; Naz, R.; Ahmad, B. Prevalent Risk of Glacial Lake Outburst Flood Hazard in the Hindu Kush–Karakoram–Himalaya region of Pakistan. *Environ. Earth Sci.* **2021**, *80*, 451. [CrossRef]
21. Ashraf, A.; Naz, R.; Roohi, R. Glacial Lake Outburst Flood Hazards in Hindukush, Karakoram and Himalayan Ranges of Pakistan: Implications and Risk Analysis. *Geomatics, Nat. Hazards Risk* **2012**, *3*, 113–132. [CrossRef]
22. Khan, I.; Ullah, A.; Zaidi, A.Z.; Panhwar, V. Assessing Glacial Lake Outburst Flood Potential Using Geospatial Techniques: A Case Study of Western Part of Gilgit-Baltistan, Pakistan. *Arabian J. Geosci*. **2023**, *16*, 49.
23. Bazai, N.A.; Cui, P.; Liu, D.; Carling, P.A.; Wang, H.; Zhang, G.; Li, Y.; Hassan, J. Glacier Surging Controls Glacier Lake Formation and Outburst Floods: The Example of the Khurdopin Glacier, Karakoram. *Global Planet. Change* **2022**, *208*, 103710. [CrossRef]
24. Mohammadi, B.; Gao, H.; Feng, Z.; Pilesjö, P.; Cheraghalizadeh, M.; Duan, Z. Simulating Glacier Mass Balance and Its Contribution to Runoff in Northern Sweden. *J. Hydrol.* **2023**, *620*, 129404. [CrossRef]
25. Pandey, P.; Banerjee, D.; Ali, S.N.; Khan, M.A.R.; Chauhan, P.; Singh, S. Simulation and Risk Assessment of a Possible Glacial Lake Outburst Flood (GLOF) in the Bhilangna Valley, Central Himalaya, India. *J. Earth Syst. Sci.* **2022**, *131*, 184. [CrossRef]
26. Singh, V.; Maurya, S.; Dey, A. The 2021 Chamoli Disaster: Is It GLOF or LLOF? In Proceedings of the North-East Research Conclave 2022, Guwahati, India, 20–22 May 2022. [CrossRef]
27. Westoby, M.J.; Glasser, N.F.; Brasington, J.; Hambrey, M.J.; Quincey, D.J.; Reynolds, J.M. Modelling Outburst Floods from Moraine-Dammed Glacial Lakes. *Earth-Sci. Rev.* **2014**, *134*, 137–159. [CrossRef]
28. Glacial Lake Outburst Floods in Nepal and Switzerland: Available online: https://www.germanwatch.org/sites/germanwatch.org/files/publication/3647.pdf (accessed on 1 November 2020).
29. Mahmood, S.; Atiq, A. Debris Flow Hazard Assessment in District Chitral, Eastern Hindu Kush, Pakistan. *Prev. Treat. Nat. Disasters* **2022**, *1*, 1–10. [CrossRef]
30. Mahmood, S. Flood Risk Modelling and Management in Panjkora Basin, Eastern Hindu Kush, Pakistan, Ph.D. Thesis, University of Peshawar, Peshawar, Pakistan, 13 November 2019.
31. Mahmood, S.; Rahman, A.U. Flash Flood Susceptibility Modeling Using Geo-Morphometric and Hydrological Approaches in Panjkora Basin, Eastern Hindu Kush, Pakistan. *Environ. Earth Sci.* **2019**, *78*, 1–16. [CrossRef]
32. Lillesand, T.; Kiefer, R.W.; Chipman, J. *Remote sensing and image interpretation*, 7th ed.; John Wiley & Sons: Hoboken, NJ, USA, 2015; 653p.

33. Iqbal, M.Z.; Iqbal, M.J. Land Use Detection Using Remote Sensing and GIS (A Case Study of Rawalpindi Division). *Am. J. Remote Sens.* **2018**, *6*, 39–51. [CrossRef]
34. Srivastava, P.K.; Han, D.; Rico-Ramirez, M.A.; Bray, M.; Islam, T. Selection of Classification Techniques for Land Use/Land Cover Change Investigation. *Adv. Space Res.* **2012**, *50*, 1250–1265. [CrossRef]
35. Hewitt, K.; Hewitt, K. Karakoram Glaciers and Climate Change. In *Glaciers of the Karakoram Himalaya: Glacial Environments, Processes, Hazards and Resources*, 1st ed.; Hewitt, K., Ed.; Springer: Dordrecht, Netherlands, 2014; 291–326. [CrossRef]
36. Sarwar, M., & Mahmood, S. Exploring Potential Glacial Lakes Using Geo-Spatial Techniques in Eastern Hindu Kush Region, Pakistan. *Nat. Hazards Res.* **2024**, *4*, 56–61. [CrossRef]
37. Kaushik, H.; Ramanathan, A.L.; Soheb, M.; Shamurailatpam, M.S.; Biswal, K.; Mandal, A.; Singh, C. Climate Change-Induced High-Altitude Lake: Hydrochemistry and Area Changes of a Moraine-Dammed Lake in Leh-Ladakh. *Acta Geophy.* **2019**, *69*, 2377–2391. [CrossRef]
38. Advance in Hydrological Engineering, Unsteady Flow Hydrulics Modle of Lower Columbia River System. Available online: http://www.hec.usace.army.mil (accessed on 15 November 2021).
39. Kalita, N; Bora, A.K. Flood Inundation Mapping In Belsiri River Basin Linking HEC-RAS and HEC-GeoRAS Model and Flood Frequency Analysis. *Int. J. Lakes Rivers* **2024**, *17*, 47–55.
40. Wang, W.; Gao, Y.; Anacona, P.I.; Lei, Y.; Xiang, Y.; Zhang, G.; Li, S.; Lu, A. Integrated Hazard Assessment of Cirenmaco Glacial Lake in Zhangzangbo Valley, Central Himalayas. *Geomorphology* **2018**, *306*, 292–305. [CrossRef]
41. Water Resources Research Report. City of London: Vulnerability of Infrastructure to Climate Change. Available online: https://ir.lib.uwo.ca/wrrr/33/ (accessed on 12 March 2023).